

# Large-Signal Behavioral Model of a Packaged RF Amplifier Based on QPSK-Like Multisine Measurements

Maciej Myslinski<sup>1</sup>, Dominique Schreurs<sup>1</sup>, Kate A. Remley<sup>2</sup>,  
Michael D. McKinley<sup>2</sup>, Bart Nauwelaers<sup>1</sup>

<sup>1</sup>K.U.Leuven, Div. ESAT-TELEMIC, Kasteelpark Arenberg 10, B-3001 Leuven, Belgium  
e-mail: maciej.myslinski@esat.kuleuven.ac.be; phone: +32-16-321117; fax: +32-16-321986

<sup>2</sup>National Institute of Standards and Technology, Electromagnetics Division, 325 Broadway, Boulder, CO 80305, USA  
e-mail: remley@boulder.nist.gov; phone: +1-303-497-3652, fax: +1-303-497-3970

**Abstract** — This work presents a large-signal time-domain behavioral model of an off-the-shelf RF amplifier based on a multisine excitation that emulates a quadrature phase-shift keyed (QPSK) signal. The multisine has been designed using an automated procedure. As a result, the excitation's Probability Density Function (PDF) approximates that of a realistic QPSK-modulated digital signal. The model accurately predicts both amplitude and phase of the complex envelope around the carrier as well as higher harmonics.

## I. INTRODUCTION

Large-signal time-domain behavioral modeling has proved to be effective in modeling amplifiers for modern wireless communication systems design [1]-[2]. This technique is based on large-signal measurements, which provide information about the behavior of the modeled component in the presence of a realistic RF excitation [3]. The measurement-based nature of this method implies that the accuracy and valid operating range of the resulting model relies largely on proper experiment design. In previous works we showed that more efficient experiment design could be achieved by replacing single-tone excitation with a multisine [4]-[5]. However the large number of possible multisine-parameter combinations leads to the problem of designing the optimal band-pass multisine signal [6] and has impact on the behavioral model extraction and validation [7,8]. In [7,8], it was shown that the statistical properties of the synthesized multisine signal are more important than the range of instantaneous amplitudes. Therefore the authors in [7,8] proposed a method to construct a multisine with a desired PDF.

In this work we apply a similar procedure to shape the PDF of the multisine, but we go one step further and employ this excitation in the large-signal measurement set-up. Unlike [7,8], we use the measured data to extract the behavioral model. For the first time a multisine excitation with a QPSK-shaped PDF is used to extract the measurement-based large-signal behavioral model of a memoryless RF amplifier. This is a more realistic excitation than in our previous works [4]-[5], where simple and generic multisines were studied. In Section II we present the outline of the modeling procedure, while Section III contains the experiment design.

Measurements and simulations that incorporate our model for a packaged buffer amplifier developed for 4.9 GHz wireless applications are compared in Section IV.

## II. OVERVIEW OF THE MODELING PROCEDURE

The behavioral modeling method used in this work is equivalent to the approach reported in [1]. The terminal currents and voltages in the model formulation were replaced by traveling voltage waves, precisely distinguishing between input and output signals of the modeled two-port. Thus the dynamic equations describing the behavior of a two-port RF component with no long-term memory are stated as follows:

$$b_1(t) = f_1(a_1(t), a_2(t), \dot{a}_1(t), \dot{a}_2(t), \dots, \dot{b}_1(t), \dot{b}_2(t), \dots), \quad (1)$$

$$b_2(t) = f_2(a_1(t), a_2(t), \dot{a}_1(t), \dot{a}_2(t), \dots, \dot{b}_1(t), \dot{b}_2(t), \dots). \quad (2)$$

In equations (1) and (2),  $b_i(t)$  and  $a_i(t)$  respectively represent the scattered and incident traveling voltage waves. The superscript dots denote time derivatives. We have to determine the functional relationships  $f_1(\cdot)$  and  $f_2(\cdot)$  between the minimal set of independent variables and the scattered traveling voltage waves. Typically to accomplish this task, we employ an artificial neural network (ANN) with parameters found by optimization [9].

The most crucial step in the procedure—determining the valid operating range of the model and therefore its robustness—is the experiment design. The type and parameters of the excitation should be planned to ensure that the measured states efficiently cover the desired operating range of the model. Subsequently these measured voltage waves are used to generate the set of independent time-domain variables. The composition of this set has to be defined and is then used as the input of the single hidden-layer ANN. The ANN parameters are calculated in an optimization procedure, leading to the best fit with the scattered traveling voltage waves at the ports of the device. Finally the ANN equations are implemented in a commercial circuit simulator. The resulting component represents the extracted behavioral model and can be used in circuit design and simulation.

### III. EXPERIMENT DESIGN

As highlighted in the previous section, experiment design and its core, the excitation design, play a key role in the determination of the model's accuracy and valid operating range.

#### A. Multisine Excitation Design

The main goal in design of the multisine excitation is to construct a periodic narrow-band signal approximating a realistic digitally modulated signal. In this work we used a procedure similar to the one described in [7], allowing alteration of a generic multisine such that its PDF mimics the corresponding statistical property of a given signal. The principle is that this method modifies the PDF of the original multisine by substituting its initial time-domain amplitude values for those corresponding to a digitally modulated signal used in modern telecommunication standards. As a result of an iterative optimization procedure, we obtain a multisine with a PDF similar to that of the digitally modulated signal. Fig. 1 shows the PDF of a 1.6 MHz bandwidth QPSK-modulated digital signal (black solid trace) and the corresponding 63-tone multisine (red dotted trace).

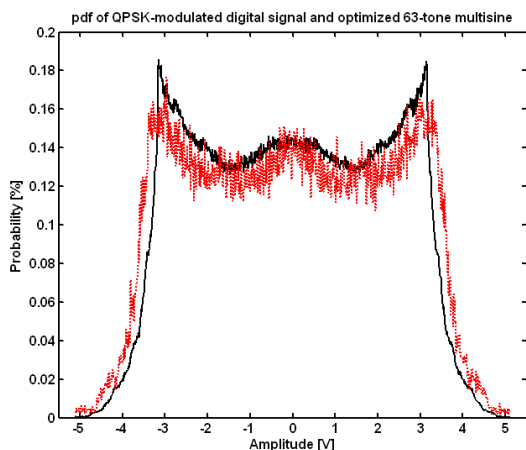


Fig. 1. PDF of a QPSK-modulated digital signal (black solid line) and optimized 63-tone multisine (red dotted line).

It is worth mentioning that the choice of the number and frequency positions of the multisine components is not straightforward and depends on the characteristics of the digital signal being considered. The detailed description of the multisine design procedure extends the scope of this article and will be reported in a future publication.

#### B. Measurements and Data Processing

The question may arise as to why the actual digitally modulated signal is not used directly, especially since this type of signal is widely available in modern vector signal generators. Unfortunately to perform credible large-signal measurements in the Large-Signal Network Analyzer (LSNA) set-up, the excitation must be periodic [3]. Therefore, the periodicity of multisines makes them well suited for this type of measurement.

The main problem encountered during measurement-data processing is the large number of time-domain data

points. This results from the large difference between the RF carrier frequency (gigahertz range) and the narrow-band multisine frequency offset (tens or hundreds of kilohertz range). The solution proposed by the authors in [4] is based on sampling the long IF period by taking every  $n^{\text{th}}$  RF period from the time-domain waveforms.

### IV. RESULTS

The modeling method described above was applied to an off-the-shelf general-purpose buffer RF amplifier developed for 4.9 GHz wireless applications. The behavioral model was extracted from the 63-tone multisine excitation with the 1.6 MHz bandwidth QPSK-shaped PDF. After implementation in the circuit simulator, the model was simulated under a multisine excitation. The signal was obtained by the same procedure as the multisine used for model extraction, but from another set of QPSK-modulated random data. Fig. 2 presents the amplitude spectra of both the multisines used for model extraction (red crosses) and for simulation (blue circles).

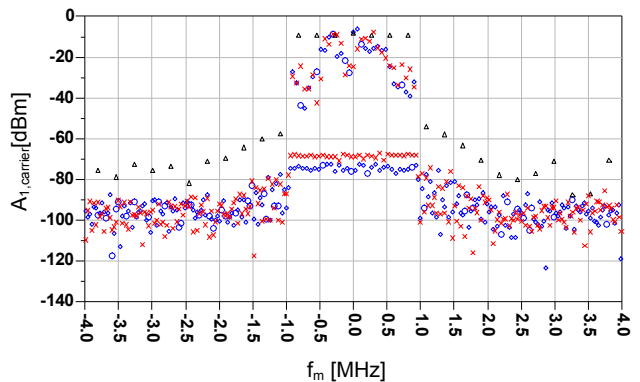


Fig. 2. Multisine excitations used for model extraction (red crosses) and simulation (blue circles), both at the carrier frequency of 4.9 GHz and  $P_{in}$  of +6 dBm. Black triangles represent multisine excitation used for the extraction of Model 2, described below.

The set of plots in Fig. 3 depicts both the time- and frequency-domain simulation results (red trace) together with the corresponding measurements (blue circles) of the  $b_2$  scattered traveling voltage wave at port 2 using the QPSK-like multisine excitation that was used to validate the model, as mentioned above. The graphs in Fig. 3(a), Fig. 3(b) and Fig. 3(c) respectively show the magnitude and phase of the complex envelope around the carrier frequency and the amplitude spectrum of this envelope. Similar results for the complex envelope around the second RF harmonic are plotted on Fig. 3(d), Fig. 3(e) and Fig. 3(f), respectively. The input power of the multisine signal was set to +6 dBm. One can notice very good agreement between the measurements and the model predictions around the RF carrier frequency as well as around its second harmonic. This confirms that the model can accurately predict the behavior around the higher order harmonics also. This ability is an important advantage over many other behavioral models, which are

‘bandwidth limited’ to the vicinity of the carrier frequency.

In addition, the influence of the realistic excitation used for extraction on the accuracy of the model prediction has been verified. For this purpose a second model has been created. This time the multisine excitation is composed of only seven tones with equal amplitudes and phases evenly distributed around 4.9 GHz in 1.6 MHz bandwidth. The amplitude spectrum of this multisine is depicted in Fig. 2 by the black triangles. For clarity, the model based on the QPSK-like multisine will be referred to as Model 1, and that based on the seven-tone multisine as Model 2.

Model 2 has been simulated under the same signal conditions as described in the case of Model 1. The resulting complex envelope of  $b_2$  traveling voltage wave around carrier frequency is shown in Fig. 4. The match between the measured waveform (blue circles) and those coming from the Model 1 (red crosses) and the Model 2 (black triangles) simulations is very good, though it is difficult to quantitatively compare the accuracy of both models predictions based only on the IQ plots of Fig. 4. This is especially true when we take into account several levels of input power.

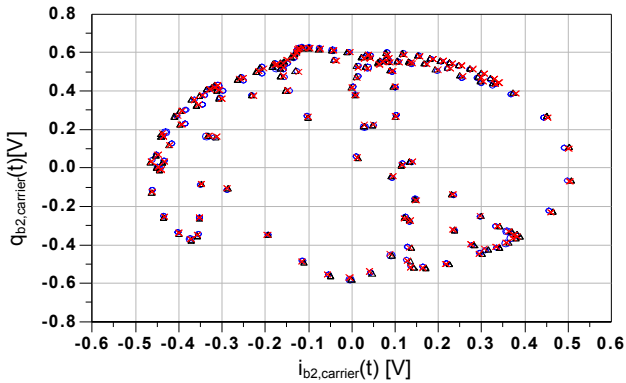


Fig. 4. IQ plot of measured  $b_2$  wave complex envelope (blue circles), simulated Model 1 (red cross) and simulated Model 2 (black triangles) at  $P_{in} = +6\text{dBm}$  and around 4.9 GHz.

Therefore, to facilitate quantitative analysis of the simulation results of both behavioral models, we propose to use an RMS error metric similar to that reported in [10]:

$$e_{k,harm} = \sqrt{\frac{\frac{1}{N} \sum_n |b_{k,harm,sim}(n) - b_{k,harm,meas}(n)|^2}{\frac{1}{N} \sum_n |b_{k,harm,meas}(n)|^2}}. \quad (3)$$

In equation (3),  $b_{k,harm,sim}$  and  $b_{k,harm,meas}$  represent the simulated and measured complex envelopes at port  $k$  and around  $harm$  (harmonic component of the carrier frequency), respectively.  $N$  and  $n$  are respectively the total number of time samples and the time sample index.

The error metric (3) has been applied to the complex envelope simulation of scattered traveling voltage waves  $b_2$  and  $b_1$  for different input power levels. The graphical representation of the results obtained is shown on Figs. 5

and 6, respectively. In both figures red line and black line with triangles correspond to the Model 1 and Model 2 metrics, respectively. One can notice that the RMS error of Model 1 prediction is smaller than the error of Model 2 for almost all investigated input power levels. This signifies the high accuracy of the model extracted from the 63-tone multisine excitation when compared with the QPSK-shaped PDF. The difference is especially visible for lower power cases.

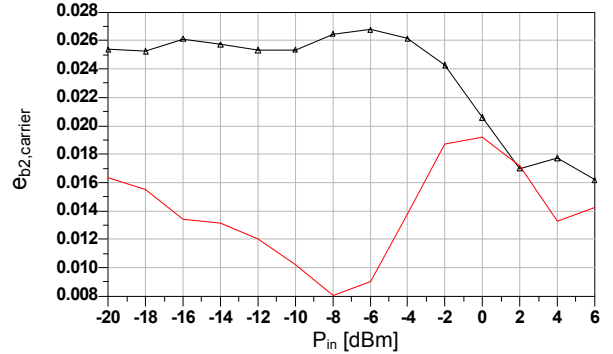


Fig. 5. RMS error metric of Model 1 (red line) and Model 2 (black line with triangles) predictions of:  $b_2$  traveling voltage wave around carrier frequency. The metric is plotted as a function of input power.

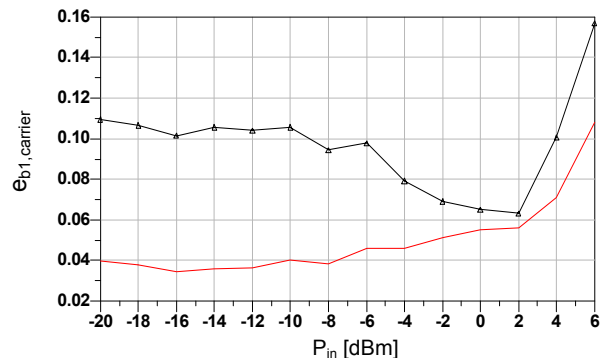


Fig. 6. RMS error metric of Model 1 (red line) and Model 2 (black line with triangles) predictions of:  $b_1$  traveling voltage wave around carrier frequency. The metric is plotted as a function of input power.

## V. CONCLUSION

In this work, we presented a method for constructing a large-signal behavioral model from a multisine with a PDF corresponding to the statistical properties of a QPSK-modulated signal to predict the behavior of an RF amplifier. We described the main steps of this successful modeling procedure and summarized the multisine excitation design method. Very good agreement between large-signal measurements and simulations both in amplitude and phase was achieved for the complex envelope not only around the carrier RF frequency but also around its second harmonic. Finally, we performed a quantitative comparison of the accuracy of the considered model and a model extracted from a simple multisine excitation.

## ACKNOWLEDGEMENT

This work was partially funded by the FWO project G.0405.03. Research reported here was performed in the context of the network TARGET– “Top Amplifier Research Groups in a European Team” and supported by the Information Society Technologies Programme of the EU under contract IST-1-507893-NOE, [www.target-net.org](http://www.target-net.org). D. Schreurs is supported by the Fund for Scientific Research-Flanders as a postdoctoral fellow. Partial work of the U.S. Government, not subject to copyright in the United States.

## REFERENCES

- [1] D. Schreurs, N. Tuffiaro, J. Wood, D. Usikov, L. Barford, and D. E. Root, “Development of time domain behavioural non-linear models for microwave devices and ICs from vectorial large-signal measurements and simulations,” in *Proceedings of the European Gallium Arsenide and related III-V compounds Applications Symposium*, pp. 236-239, October 2000.
- [2] J. Wood, “Nonlinear time series for black-box behavioral modeling of integrated circuits,” *IEEE Int. Microwave Symp. (MTT-S) Workshop on WSG: Fundamentals of Nonlinear Behavioral Modeling: Foundations and Applications*, June 2003.
- [3] J. Verspecht, P. Debie, A. Barel, and L. Martens, “Accurate on wafer measurements of phase and amplitude of the spectral components of incident and scattered voltage waves at the signal ports of a nonlinear microwave device,” *IEEE MTT-S Digest*, pp. 1029-1032, May 1995.
- [4] D. Schreurs and K. Remley, “Use of multisine signals for efficient behavioural modelling of RF circuits with short-memory effects”, *Automatic RF Techniques Group Conference*, pp. 65-72, June 2003.
- [5] D. Schreurs, M. Myslinski, and K.A. Remley, "RF behavioural modelling from multisine measurements: influence of excitation type", *European Microwave Conf. (EuMW)*, pp. 1011-1014, October 2003.
- [6] K.A. Remley, “Multisine excitation for ACPD measurements”, *IEEE Int. Microwave Symp.*, pp. 2241-2144, June 2003.
- [7] J.C. Pedro and N.B. Carvalho, “Designing Band-Pass Multisine Excitations for Microwave Behavioral Model Identification”, *IEEE MTT-S Digest*, pp. 791-794, June 2004.
- [8] J.C. Pedro and N.B. Carvalho, “Designing multisine excitations for nonlinear model testing”, *IEEE Transactions on Microwave Theory and Techniques*, Vol. 53, No. 1, pp. 45-54, Jan. 2005.
- [9] Q.J. Zhang and K.C. Gupta, *Neural networks for RF and microwave design*, Artech House, 2000.
- [10] K.A. Remley, J.A. Jargon, D. Schreurs, D.C. DeGroot, and K.C. Gupta, “Repeat Measurements and Metrics for Nonlinear Model Development”, *IEEE Int. Microwave Symp.*, pp.2169-2172, 2002.

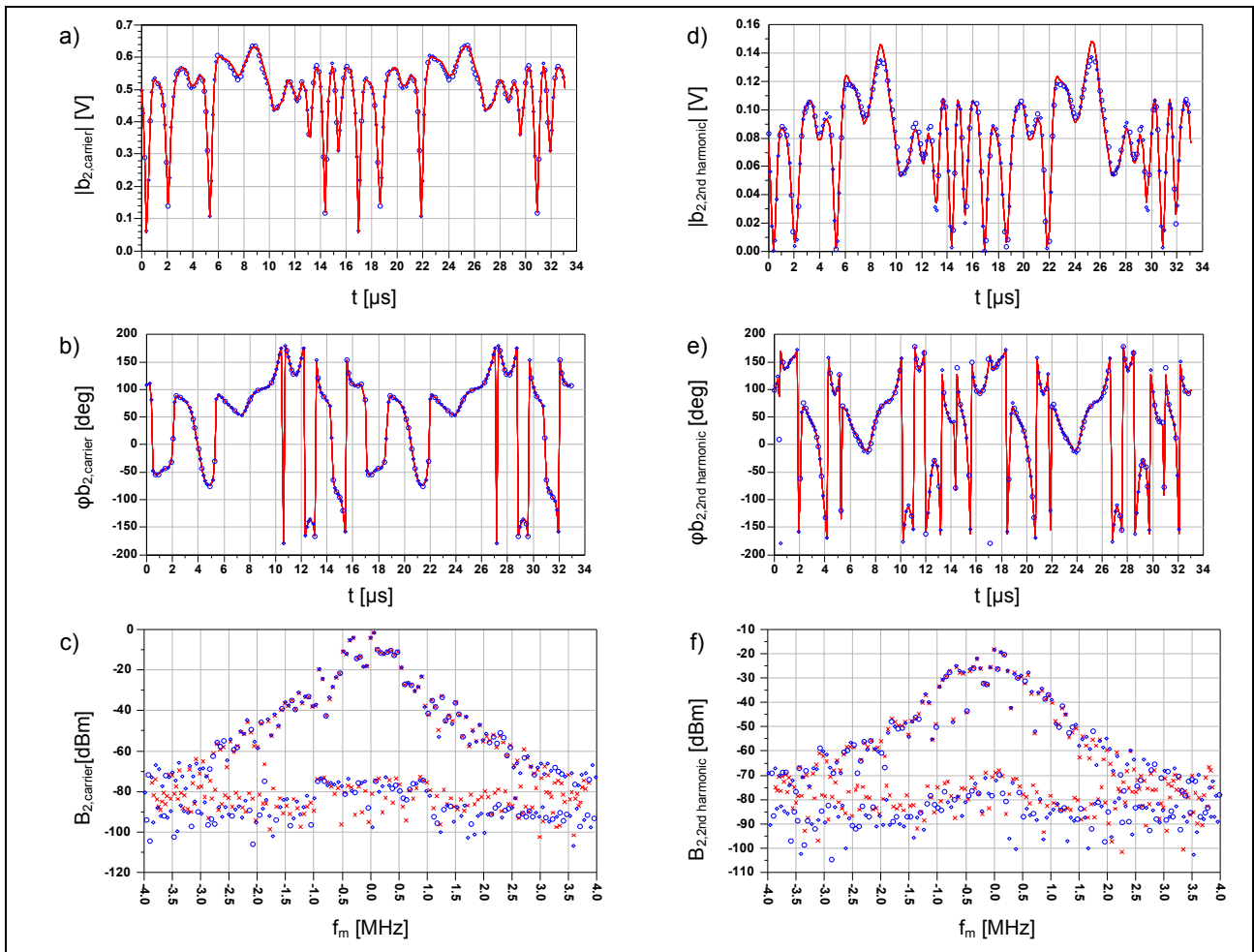


Fig. 3. The measured (blue circles) and simulated (red trace or crosses)  $b_2$  scattered traveling voltage wave: (a) magnitude waveform, (b) phase waveform, (c) amplitude spectrum of the complex envelope around RF carrier frequency 4.9 GHz, and (d) magnitude waveform, (e) phase waveform, (f) amplitude spectrum of the complex envelope around the second RF harmonic; the input power is 6 dBm.